




Urban Heat Island vulnerability mapping using advanced GIS data and tools

PARAS SIDDIQUI^{1,*} , PHILLIP B ROÖS², MURRAY HERRON², DAVID S JONES³,
EMMA DUNCAN², ALI JALALI², ZAHEER ALLAM², BRYAN J ROBERTS⁴,
ALEXANDER SCHMIDT⁵, MUHAMMAD ATIQ UR REHMAN TARIQ^{6,7},
ASHFAQ AHMED SHAH^{8,9}, NASIR ABBAS KHAN¹⁰ and MUHAMMAD IRSHAD¹¹

¹*School of Life Sciences, University of Technology Sydney (UTS), Ultimo 2000, Australia.*

²*Live+Smart Research Laboratory, School of Architecture and Built Environment, Deakin University, Geelong, VIC 3220, Australia.*

³*Cities Research Institute, Griffith University, Nathan, QLD 4111, Australia.*

⁴*Department of Environment, Land, Water, and Planning (DEWLP), Victoria State Government, Geelong, VIC 3220, Australia.*

⁵*City of Greater Geelong (COGG), Geelong, VIC 3220, Australia.*

⁶*College of Engineering and Science, Victoria University, Melbourne 8001, Australia.*

⁷*Institute for Sustainable Industries and Liveable Cities, Victoria University, P.O. Box 14428, Melbourne 8001, Australia.*

⁸*School of Public Administration, Hohai University Nanjing, Jiangsu Province, China.*

⁹*Research Centre for Environment and Society, Hohai University Nanjing, Jiangsu Province, China.*

¹⁰*School of Management Science and Engineering, Nanjing University of Information Science and Technology, Pukou District, Nanjing, Jiangsu Province, China.*

¹¹*Department of Environmental Sciences, COMSATS University Islamabad, Abbottabad Campus, Abbottabad, Pakistan.*

*Corresponding author. e-mail: parissiddiqui@gmail.com paras.siddiqui@uts.edu.au

MS received 30 November 2021; revised 15 April 2022; accepted 26 July 2022

Urban Heat Island (UHI) is a phenomenon that can cause hotspots in city areas due to dense, impervious infrastructure and minimal vegetation cover. UHI hotspots may become worse in extreme heat events that are already affecting many regions across the globe due to increased frequent hot extremes, human-induced warming in cities, and rapidly growing urbanization, as documented by the latest IPCC report 2021. In seeking to support designers, planners, and decision-makers in developing and implementing adaptation strategies and measures to make our cities sustainable and resilient, reliable projections and modelling are required. In this study, we modelled UHI vulnerability using high-resolution spatial data, advanced geospatial tools, and socio-demographic data. This modified vulnerability approach drew upon UHI index maps and 20 select customized indicators of heat exposure, population sensitivity, and mobility/adaptive capacity. The indicators were Delphi evaluated and weighted, and the methodology was applied against the City of Greater Geelong municipality in Australia. The resulting UHI index maps indicated significant hotspots in areas of high building density, commercial/industrial zones, newly constructed sites, and zones with low urban green infrastructure. These UHI maps, in combination with selected indicators, highlighted the areal concentration of heat risk areas and vulnerable locations for the sensitive human population. The highlighted areas were primarily concentrated in high building density and high population density areas, which was seen through correlation curves. However, the building

density showed a weak correlation, and population per meshblock indicated a strong correlation with UHI measurements. This study provides a comprehensive analysis of risk mapping and vulnerability assessment using GIS geospatial data for the advancement of a major local government area and concludes that this methodology has replicability incomparable geographical regions.

Keywords. UHI; heatwave; risk and vulnerability maps; Greater Geelong; GIS.

1. Introduction

As evidenced in Intergovernmental Panel on Climate Change (IPCC) reports published in 2018, human-induced climate change has been reported to be affecting climate and weather extremes around the globe with increased frequency of extreme events, including heatwaves, heavy rainfalls, droughts, and tropical cyclones (Masson-Delmotte *et al.* 2018). IPCC 2021 reports that human-induced climate change is already affecting many regions across the globe with increased heatwave events, floods, and droughts (IPCC 2021). The report further details global surface temperatures to be 1.09°C higher between 2011 and 2020, higher than the temperature rise reported between 1850 and 1900. IPCC 2021 reported that human-induced climate change has already been affecting many regions across the globe with increased heatwave events, floods, and droughts. Human-induced warmings have been intensified locally in cities, and further frequent hot extremes with growing urbanization are leading to the severity of heat waves (IPCC 2021). Increases in the intensity of heat waves will be concentrated more in cities than rural or peri-urban areas since urban areas already experience increased temperatures due to the urban heat island (UHI) effect (Sidiqi *et al.* 2016; Rizvi *et al.* 2019).

The ‘Urban Heat Island’ (UHI) effect is the phenomenon where cities show a higher temperature than their surrounding non-built areas. Based on UHI theory, cities tend to have higher surface and air temperatures than adjacent rural zones. The UHI is caused due to landscape modifications, high densities of impervious or impermeable surfaces, and less percentage cover of green vegetated areas in urban zones. The UHIs are deleterious modifications in the environment that result in increased temperatures in urban zones compared to rural or non-built areas. Most cities are surrounded by green vegetated zones or peri-urban agriculture land that contrasts and concentrates UHIs in cities due to their absence of vegetation cover or little

greenness compared in urban zones to surroundings (Keeratikasikorn and Bonafoni 2018). The factors that affect the temporal and spatial variability of UHI are many; however, the vegetation cover type and impervious surface play the most crucial role. The vegetation plays a role in driving the inter and intra-annual patterns in UHI. The vegetation also derives the daytime UHI by providing cooler surfaces via evapotranspiration. On the other hand, the impervious surfaces drive night-time UHI trends due to the high thermal inertia characteristics of given materials. Therefore, the gradient in vegetation cover from rural to urban zones causes spatial variability in temperature and gives rise to the UHI effect. It also gives rise to temporal variability in UHI intensity over the year. However, these seasonal, temporal, and diurnal characteristics of UHI are out of scope for a given study. The effects of UHI on cities across the globe cannot be overemphasized, particularly in exacerbating negative impacts on urban residents’ health, ecological environment, economy, energy, social well-being, and others. In urban ecology, UHI has been observed to be negative influential, resulting in higher air and water pollution levels as reported in cities including Athens (Keramitsoglou *et al.* 2011), Paris (Menut 2000), Berlin (Li *et al.* 2018), Taichung City (Lai and Cheng 2009), and Port Louis (Zaheer and Elahee 2014). On human health, this urban phenomenon has been reported as causing respiratory difficulties, heat cramps, physical discomforts, and other health issues resulting in increased morbidity rates (Vaidyanathan *et al.* 2020). In extreme cases, UHI has been reported as heightening mental illness and in worse-case scenarios, deaths (Tomlinson *et al.* 2011; Heaviside *et al.* 2017). On this, in United States, there is evidence of over 10,527 deaths between 2004 and 2018 arising from heat-related complications (Vaidyanathan *et al.* 2020). In Pakistan and India, 3500 deaths are documented as being associated with a heatwave in 2015 (Saeed *et al.* 2021). This global health burden has, in most cases, resulted in a direct ‘assault’ upon host economies with

increased hospitalization and medication costs. For instance, a study estimated that in New York, every year, an amount of more than US\$ 644,069 is spent to cater for hospitalization of such cases (Lin *et al.* 2012). UHI is also credited with increasing urban energy demand, especially in air-conditioning technologies (Raalte *et al.* 2012; Héliá and Graham 2015). Noting that a majority of energy sources are from non-renewable energy sources, this has a direct effect on increasing carbon emissions. Arising from excessive heat instances, an increasing urban budget is expended upon the renewable energy sector. For instance, in Melbourne, it is reported that approximately AU\$ 1.8 billion is spent on heat mediation activities, with over AU\$ 300 million attributed directly to UHI18. In European cities, Costa and Floaster (Héliá and Graham 2015) report that when there are unit increases in temperatures, especially during summer, there is a proportionate increase of approximately 1.66% in energy consumption which translates to between AU\$ 382.67 million (€314) to AU\$ 28,035.20 (€23,004) million in a year used for the different preventative and containment measures. The cumulative impacts of UHI on different sectors are particularly sharp in the economic sector (Walter 2016). Cities reporting high incidences of UHI are equally witnessing high economic costs and diversion of economic resources from development agendas to preventive and mitigation programs against this menace. The costs of investing in infrastructures that can withstand and alleviate some of the challenges caused by UHI are also high, and their ramifications are experienced in the entirety of a city, warranting the need to undertake this study.

Geospatial tools in mapping UHI offer advanced remote sensing/airborne data and spatial analytics to process huge datasets efficiently. Remote sensing has capabilities to capture wider areas and has to offer a huge archive of data that allows users to go back in time and collect the data as required. The air temperature data available from observatories are mostly limited to the number of stations available. The analysis gets limited not only in time but also in terms of spatial pattern analysis. On the other hand, remote sensing and geospatial tools allow the user to investigate larger spatial areas with great temporal coverage.

For Australian cities, it is noted that they are prone to persistent risks due to variations in climate change and projected rise in incidents of extreme weather events. In Australia, surface temperatures have increased by 1°C since 1910 (Grose 2015;

BOM 2017). The 11-year mean temperature for 2008–2018 was a record high, approximately 0.77°C above the average (BOM 2018). Warming remained modest in Australia during the early 20th century, with a slight drop from 1935 to 1950, and then it rapidly increased (CSIRO 2011). Almost all of the Australian continent has warmed over the last 50 years since 1960 (CSIRO 2011). Most Australian regions have experienced a temperature rise of up to 2°C over the last 50 years, while others have experienced little or no change (CSIRO 2011). The number of days with record hot temperatures has increased each decade over the past 50 years (CSIRO 2011). It is further reported that the strongest trends in the frequency of hot days and warm nights have occurred in the tropical northeast of Australia since the mid-20th century, while the most substantial declines in the frequency of cold days have occurred across its southern flanks (Sidiqi *et al.* 2016). Thus, with existing UHIs in urban areas, increased frequencies of extreme temperature events may elevate the risk factors for the resident human population and result in loss of human lives due to extreme heat incidents or heat-related illnesses along with existing hotspots in urban zones. In 2009, 173 people died in the Black Saturday bushfires in the state of Victoria; however, more than twice as many victims lost their lives in the heatwave that preceded these fires (Black Saturday death toll lowered – ABC News (no date)). In Victoria, heatwave events in 2008, 2009, and 2014 caused 101, 374, and 167 deaths, respectively, according to reports published Victorian Auditor-General (Heatwave Management: Reducing the Risk to Public Health | Victorian Auditor-General's Office (no date)). They concluded that the greatest number of deaths occurred in people 75 years of age or older (DHS 2009). The human mortality associated with heatwaves can be considerable, but there are important unresolved questions about the extent to which deaths are brought forward in time and the extent to which many of these deaths are preventable (Kovats and Kristie 2006). The January 2009 heatwave in Victoria was of unprecedented intensity and duration, with maximum temperatures 12–15°C above normal average across much of the Victorian state, including its capital Melbourne (DHS 2009). During the Summer week of 26 January to 1 February 2009, medical locum services attended to 96 patients diagnosed with direct heat-related effects, including heatstroke, heat stress, heat exhaustion, heat syncope, heat rash, and dehydration. According to the

Australian Bureau of Meteorology (BOM), the summer of 2016–2017 in Australia broke more than 205 climate records and included several extreme temperatures in January and February (ABC 2009). In January and February 2017, southeastern Australia was hit by a series of distinct heatwaves, with the deadliest one being recorded in the period 9–12 February 2017 (ABC 2009). This event, in addition to other such past events, demonstrates the heightened urgency to undertake city-level heat-related climate change mapping, conducting detailed analysis, and scenario model the risks of extreme heat events upon our vulnerable human populations, especially those living in cities.

2. Background

There are various methods and approaches that can be adapted to analyze and map UHI. Traditionally, the most potent approach is the reliance on data and information drawn from satellites, as practised by NASA (Zhou 2018). The data can also be obtained from sources including the National Centers for Environmental Information (NOAA), the National Weather Service Stations, and National Centres for Environmental Prediction, and NASA's Moderate Resolution Imaging Spectroradiometer (MODIS), among others (Galloa *et al.* 1993; Schatz and Kucharik 2015; Mathew *et al.* 2019). However, with time, other methodologies, including remote sensing, use of GIS-based spatial analysis, and relying on unmanned aerial systems (UAS) (like the use of unmanned aerial vehicles (UAVs)), have emerged, opening the scope and capabilities of mapping and analyzing. In most cases, a combination of both the traditional and modern approaches is adopted by researchers to map, analyze and evaluate the effects of UHI. Stelian applied this approach in their analysis of the effects of UHI in the city of Sofia, Bulgaria (Dimitrov *et al.* 2020). Wang notes that the use of remote sensing, among other modern methodologies, can help in solving some obvious flaws that are synonymous with conventional UHI monitoring methods (Wang *et al.* 2019). The key advantage of adopting modern technologies is that they can be seamlessly combined and used together, thereby helping to include diverse variables and indicators such as land covers, temperatures, and others.

Data from networks of meteorological observation stations have also been a potential source of data for mapping UHI, especially in the United

Kingdom (Chowienczyk *et al.* 2020). While all these methodologies are important, they need to capture different variables and indicators to ensure that they not only help in identifying UHI but also in identifying vulnerability and risks. The need for a wide scope of variables is important as it can help in the generation of a UHI map, which has not always been the case with most studies conducted. In most cases, temperature maps and grid maps are most common, but in the case where multiple methodologies are combined, more variables can be introduced, including UHI mapping and analysis, rendering more accurate information leading to informed policy decisions.

In our literature appraisal, mapped in table 1, only a few studies were identified that propose various methods and indicators for mapping and analyzing urban heat vulnerability risks. Such research is highlighted in the literature that was based upon past and recent developments in mapping and monitoring heat risk to vulnerable populations in city areas. Table 1 thus coalesces a group of current and relevant studies that have been conducted around the world in various cities to examine and review their methodologies, analyses, and parameters/indicators applied in their attempts to identify UHI vulnerability and risk at various scales.

Despite their different approaches, shortcomings in all of these studies were the nature of risk factors applied to measure and evaluate heat exposure, sensitivity, and adaptive capacity. These multiple studies used various risk factors, predominately utilizing simple temperature maps to identify heat exposure in urban zones. However, UHI is one phenomenon that may cause hot spots in urban areas, causing particular and discrete locations to be at relatively higher risk than other zones within the same urban polygon. Therefore, a broad-brush approach was infeasible and lacked the quality resolution to inform conclusions.

Moreover, none of the above studies utilized UHI index maps to identify heat exposures within a city block. Instead, most studies used temperature maps only to characterize locations prone to extreme heat. UHI is an index that is calculated by subtracting urban temperature from non-urban temperatures. With advancements in spatial science and tools, it has become increasingly possible to map UHI footprints at local and neighbourhood scales, or census districts (CD) and at meshblock levels in Australia. This research further identifies and appraises the levels of resilience of those humans who are most vulnerable in this municipality from a social

Table 1. Indicators as identified from the literature.

	Indicators	Literature review	Description
Population sensitive to heat	Children <5	Räsänen and Heikkinen; Rizwan; Sanchez and Reames;	Population factors that may cause people to be more
	Elderly >65	Méndez-Lázaro, Vargo, Chuang and Gober, Lemonsu;	vulnerable to heat risk by reducing their ability to
	Ill-health/people with disabilities (%)	Heaton and Sain; Huang; Uejio and Wilhelm; Reid	thermoregulate, resulting in illness leading to deaths.
	People taking medication (asthma, heart disease, diabetes)	and O'Neill (Reid <i>et al.</i> 2009; Uejio <i>et al.</i> 2011; Heaton	Certain populations tend to be more vulnerable due to
	Gender (women)	<i>et al.</i> 2014; Chuang and Gober 2015; Lemonsu <i>et al.</i>	factors such as age, illness, low income, etc. These
	Poor social networks (unemployment rate) and homeless people	2015; Vargo <i>et al.</i> 2016; Méndez-Lázaro <i>et al.</i> 2018;	factors can be identified as significant indicators to
	Weak economic status (low income)	Räsänen <i>et al.</i> 2019; Sanchez and Reames 2019; Yang	map the heat stress and heat vulnerable population in
	Low level of education	<i>et al.</i> 2019)	cities.
	Immigration or race		
	Poor social networks (unemployment rate)		
Mobility/accessibility to thermal comfort	People living alone (%)		
	Linguistically isolated households (%)		
	Zones with a relatively higher population density		
	Hospitals	Li; Epstein (Epstein and Atul 2006; Li <i>et al.</i> 2020)	Access to medical facilities (emergency services).
	Ambulance		
	Medical centres		
	Per cent green space or green infrastructure	AECOM; Meerow and Newell; Reid and O'Neill; Harlan	Various attributes of land use and land cover may play
	Impervious surface (%)	and Brazel; Chow; Uejio and Wilhelm; Harlan and	an essential role in thermal comfort or reducing the
	Shopping centres/cinemas	Brazel; Meerow and Newell; Wang; Heaton; Harlan	heat stress of the population nearby.
	Community centre/care	and Brazel; Sharma (Harlan <i>et al.</i> 2006; Reid <i>et al.</i>	
Open spaces	2009; Uejio <i>et al.</i> 2011; Chow <i>et al.</i> 2012; Raalte <i>et al.</i>		
Public transport/bus stops/train stops	2012; Heaton <i>et al.</i> 2014; Meerow and Newell 2017;		
Buildings with air conditioning	Sharma <i>et al.</i> 2018; Wang <i>et al.</i> 2019)		
Swimming pools			
Quality of the built environment			

Table 1. (Continued.)

	Indicators	Literature review	Description
Heat exposure	Air quality	Voelkel and Hellman; Kumar and Geneletti; Uejio and Wilhelm; Harlan and Braze; Meerow and Newell (Harlan <i>et al.</i> 2006; Uejio <i>et al.</i> 2011; Kumar <i>et al.</i> 2016; Meerow and Newell 2017; Voelkel <i>et al.</i> 2018)	Hot days per year. Mean temperature increase and several heavy rains.
	Air temperature	Sidiqui; Meerow and Newell; Sidiqui; Huang; Uejio; Oke (Oke 1982; Huang <i>et al.</i> 2011; Uejio <i>et al.</i> 2011; Sidiqui <i>et al.</i> 2016; Meerow and Newell 2017; Sidiqui <i>et al.</i> 2022)	Urban hotspots that may cause the city to be at high risk from heat or extreme temperatures; High-resolution traffic-related air pollution estimates.
	Humidity	Kumar and Geneletti; Harlan and Brazel (Harlan <i>et al.</i> 2006; Kumar <i>et al.</i> 2016)	Green space per person.
	Vapour pressure	Wang; Méndez-Lázaro (Méndez-Lázaro <i>et al.</i> 2018; Wang <i>et al.</i> 2019)	Percent cover of roads, high-density areas, and buildings as per land use land cover data that may give information on total impervious surface cover.
	Precipitation		
	Land surface temperature (LST maps)		
	Air temperature data		
	Greenness cover		
	Impervious surface (%)		

perspective to the impacts of Urban Heat Island (UHI). For which data images of summer (representing hottest summer days in concurrent years) were acquired and processed. The process further identifies 20 potential population sensitivity, mobility, and heat exposure indicators. These indicators are adjusted and selected based on literature and outcomes of multiple workshops organized with the city council, emergency department, health department, and state government.

In this study, we mapped UHI using Landsat imagery and thermal imagery from drones for the City of Greater Geelong (COGG), the largest regional city in Victoria outside Melbourne and a city that is encompassed within one large expansive municipality. These UHI maps were then integrated into our heat vulnerability index analysis. The UHI vulnerability analysis was carried out on the basis of three main factors: (1) sensitivity, (2) adaption (mobility/accessibility), and (3) exposure to heat.

To achieve this outcome, we integrated geospatial data with socio-demographic data to map and create a detailed and interactive Urban Heat Vulnerability (UHV) mapping and monitoring for the COGG. The methodology was divided into two parts: (a) analyzing existing urban heat island (UHI) patterns across the city and (b) generating a detailed CD-level and meshblock-level UHV analysis for COGG.

To investigate and incorporate how climate change was and is going to impact the risk and vulnerability of humans in a city urban planning zone and each CD-level and meshblock-level, we defined and mapped the UHV and tried to understand its relationship with building density and population spread.

The objectives of this research were to:

- identify independent standard and custom indicators and weigh each indicator according to their contribution to the risk and vulnerability of sensitive populations;
- identify hotspots in the city experiencing the urban heat island effect;
- integrate heat maps with identified indicators to generate detailed UHV maps for the study area with a CD-level and a meshblock-level resolution.

2.1 Study area

The city of Greater Geelong is Australia's one of the fastest-growing regional cities. The city is

geographically located near the south of Melbourne in Australia. The population of Geelong is approximately 260,000, which is forecasted to grow to 393,200 by 2041 with a growth rate of 1.44% (Western Geelong Growth Area Precinct – VPA 2022). The climate of Geelong is a temperate and warm climate. The city experiences an annual mean temperature and precipitation of 14.7°C and 522 mm, respectively (Roös *et al.* 2021). Figure 1 shows the study area.

Geelong has remained a regional town over the past; however, with recent population rise and development, the town has become a regional centre with a population climbing faster than almost anywhere else in Australia, and the recent covid-19 pandemic has only added to the demand (Clayton 2021). In recent years, Geelong has been reported to be grown at the most significant growth rate among Australia’s capital cities, with a rate of 14% over the past five years (Fastest Growth Region Needs Faster Infrastructure Delivery – G21 2020). Furthermore, the growth areas in Geelong are further set to contribute to the largest urban growth in regional Victoria, with the potential to welcome more than 100,000 residents in growth area Precinct Structure Plans (PSPs) (Western Geelong Growth Area Precinct 2022). On the other hand, it is known that climate change, rising global temperatures, and droughts are already existing climate issues in all regions across the globe, as per the recent IPCC report (Intergovernmental Panel on Climate Change (IPCC) 2021). With a rising

population, urban heat may present social, economic, and environmental risks. These may further be exacerbated by extreme climate events such as heatwaves in the region. The present study analyses the risk maps for Geelong in the context of existing UHI and other sensitivity factors. Since the city is moving faster in development and growth, this study presents an excellent example of mapping and monitoring risk to make future development more sustainable and liveable.

2.2 Data and methods

The data acquired was prepared to construct indicators based on three factors:

- (1) population sensitivity to heat and socio-economic variables that may increase risk factors;
- (2) mobility/accessibility to thermal comfort zones or medical facilities;
- (3) spatial locations that were relatively more prone to heat exposure due to existing urban hot spots or minimal greenness cover or possessing a high impervious percentage of surfaces (Rinner *et al.* 2010; Räsänen *et al.* 2019).

Figure 2 summarises the proposed conceptual diagram for UHV mapping. Figure 3 further splits up the conceptual diagram explaining the detail of representations or data acquisition on selected themes and workflow.

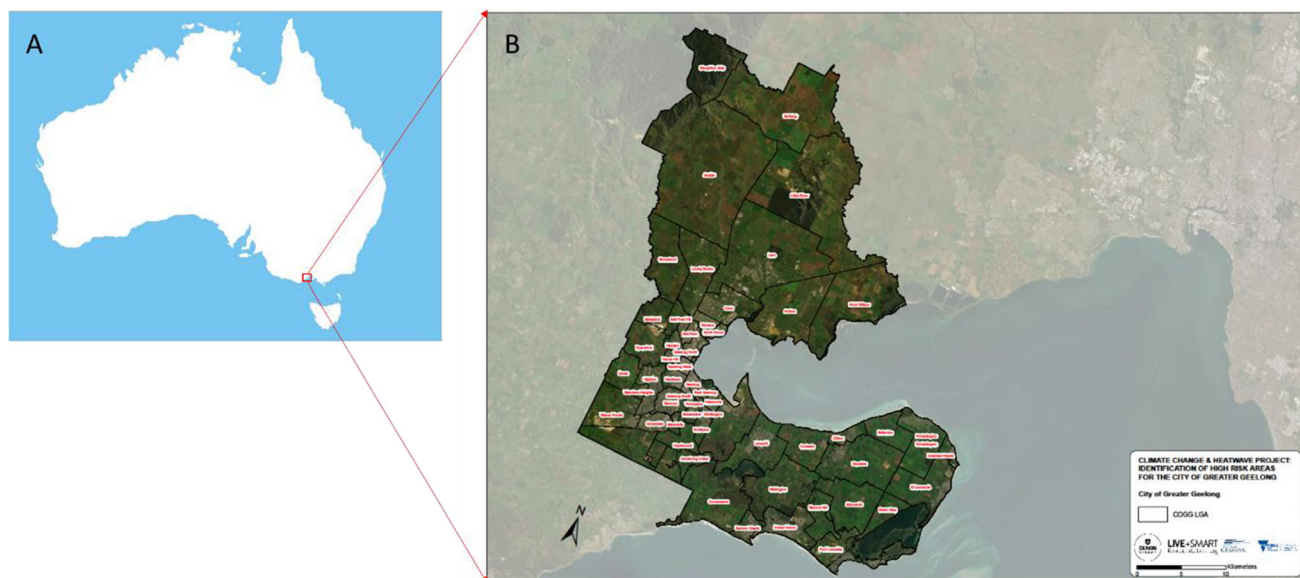


Figure 1. The city of Greater Geelong, as seen from the satellite image. (A) Australia as seen on the world map, the small red box illustrates the study area; (B) Satellite image of the study area in true colour (modified from Roös *et al.* 2021).

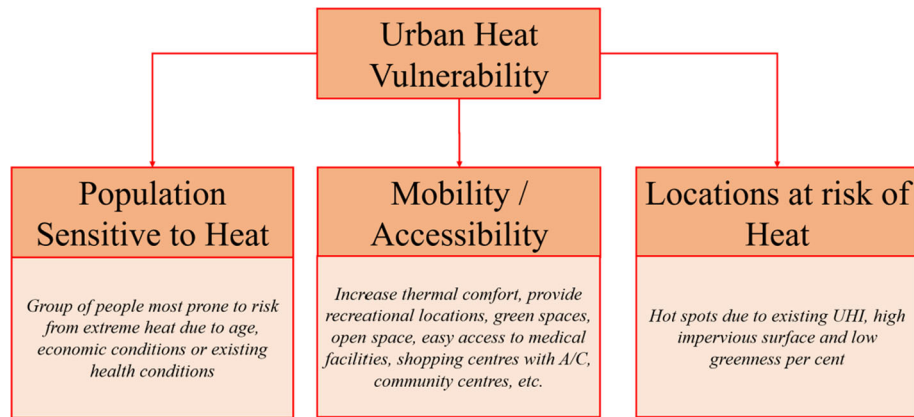


Figure 2. Conceptual diagram of heat.

3. Preparation of data

3.1 Socio-economic and socio-demographic data

In terms of socio-economic data, information about population, age groups, people with health issues, people living in isolation, people with low economic conditions, and gender information were downloaded and assembled from the Australian Bureau of Statistics (ABS) 2016 records (<https://www.abs.gov.au>). ABS offers data as per meshblocks derived from the Australian Statistical Geography Standard (ASGS) Volume 1. Meshblocks are the smallest geographical area defined by ABS, smaller than CDs, and form the building blocks for the larger regions of the ASGS. All other statistical areas or regions are built up from or approximated by whole meshblocks. They broadly identify land use such as residential, commercial, primary production and parks, etc.

3.2 Other ancillary data

In terms of GIS Data, detailed specific data on cadastre, land use and land cover, and building usage, including community centres, medical centres, hospitals, ambulance shelters, bus shelters, train stations, road network data, vegetation, and green areas coverage data, street tree, public open space, tree species data, general open space data, and building blocks were collected in the form of GIS layers. These datasets were extracted at meshblock level from local data distributing government/semi-government agencies.

The files on vegetation and open spaces included attributes on vegetation type, such as trees, forest, woodlands, parks/grasslands, shrubs, coastal

vegetation, dry land vegetation, recreational areas, nature conservation, passive outdoor enjoyment, and places of public gatherings.

3.3 Satellite and airborne data

3.3.1 Landsat data

Landsat data along with airborne thermal data were used to map UHI footprints and intensity at the neighbourhood scale. Data belongs to the Landsat-8 satellite. The Landsat-8 data offers a spatial resolution of 100 m for thermal bands. Landsat has a temporal resolution of 16 days. Landsat data can be obtained from the Earth Resources Observation and Science (EROS) Centre (www.espa.cr.usgs.gov/). Data in this study were from the Landsat Thermal and Infrared Sensor (TIRS, Landsat 8) with 16 days of temporal and 100 m spatial resolution. Amongst all the available data from 2015 to 2019, the images with less than 5% cloud cover for the Australian summer season (November, December, and January) were chosen. The data selection was done based on availability in the data catalog, cloud coverage, clear visibility, and days of extreme heat events as per records and local newspaper articles. The Landsat scenes were of the dates 11-11-2017, 15-12-2017, and 12-12-2016, which were mentioned to be the hottest days of summer for selected years as documented in local reports and news media. The thermal bands were converted into brightness temperature measures and then into land surface temperature measures using the single-channel (SC) approach (Li *et al.* 2013). The LST data was later converted into urban heat island (UHI) data using algorithms successfully

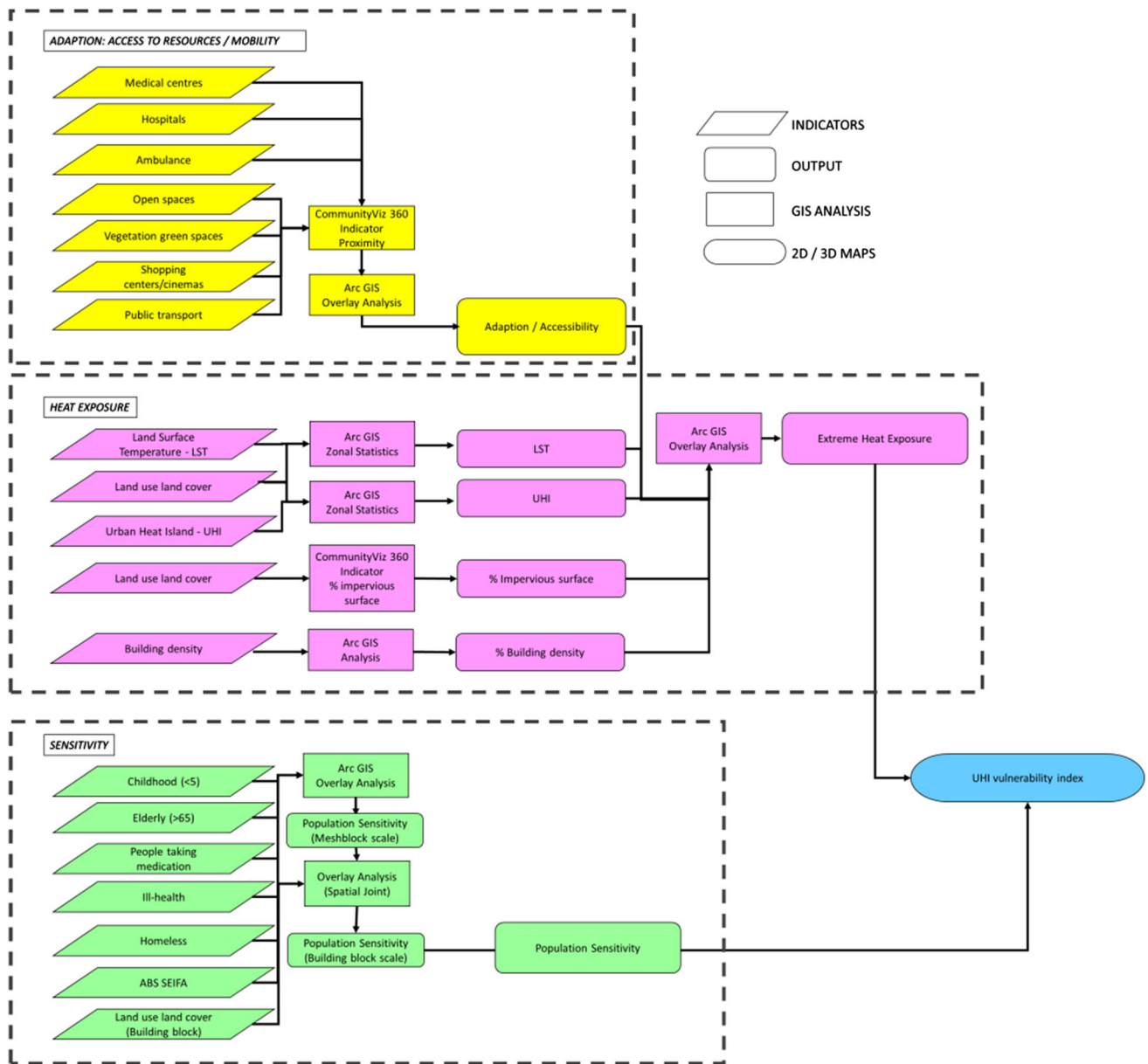


Figure 3. Detailed conceptual diagram of heat vulnerability (source: modified from Roös *et al.* 2021).

applied (Oke 1982; Voogt and Oke 2003; Sidiqi *et al.* 2016, 2022).

3.3.2 Aerial imagery data

For aerial photos, data with a spatial resolution of 0.5 m was acquired from COGG for the month of September 2018. The datasets were provided in Kelvin (K) unit and then converted into degrees Celsius (°C) for analysis. K, a unit of thermodynamic temperature, comprises the fraction $1/273.16$ of the thermodynamic temperature of the triple point of water, being: $t = T - T_0$. $t/°C = T/K - 273.15$. The K and the degree °C are also the

International Temperature Scale of 1990 (ITS-90) units adopted by the International Committee for Weights and Measures (CIPM) in 1989. Later we calculated UHI on this data using algorithms (Oke 1982; Sidiqi *et al.* 2016).

3.3.3 Data validity/ground truthing

All datasets, including (satellite images, airborne thermal imagery, land use land cover data, vegetation data, and other ancillary data) were ground-truthed by the council. Moreover, the vector files, such as land use/land cover, vegetation files, etc., were also highly detailed. The council did the

ground-truthing of data to ensure that the data provided to its stakeholders was smooth and dependable.

3.3.4 UHI plots

To understand the spatial extent of UHI and its variation in space, we followed the following method to map UHI (Lee *et al.* 2013; Siddiqui *et al.* 2016; Keeratikasikorn and Bonafoni 2018; Siddiqui 2019). The process of extracting UHI was applied to both the landsat image and aerial photo. To calculate UHI, we first marked out urban zones from the LST image of the study area, leaving only rural pixels in the image. The urban and rural pixels were identified using land use/land cover data, secondly, calculated the mean over rural pixels. Thirdly, the rural LST mean was then subtracted from the original LST images to calculate UHI (equation 1). The UHIs mapped from satellite and aerial photo, were then averaged to make a final footprint of UHI for incorporation into UHV analysis.

$$\text{UHI}(x, y) = \text{LST}(x, y)_{\text{original}} - \text{LST}(x, y)_{\text{rural}}$$

(Voogt and Oke 2003; Siddiqui *et al.* 2016; Siddiqui 2019) (1)

where (x, y) represents the coordinate of single-pixel, $\text{LST}(x, y)_{\text{original}}$, $\text{LST}(x, y)_{\text{rural}}$, and $\text{UHI}(x, y)$ represent original LST measurement, and isolated UHI intensity at x, y pixel positions, respectively.

3.3.5 Identifying key indicators for UHV mapping

The data acquired was prepared to construct the indicators based on the following three factors:

- (1) population sensitivity to heat and socio-economic variables that may increase the risk factors;
- (2) mobility/accessibility to thermal comfort zones or medical facilities;
- (3) spatial locations that were relatively more prone to heat exposure due to existing urban hotspots or less greenness coverage or possessing a high impervious percentage surface (Rinner *et al.* 2010; Räsänen *et al.* 2019).

These datasets were utilized to construct the required indicators to generate the risk factors for exposure and sensitivity of the vulnerable population to heat. The indicators were identified and

weighted based on a Delphi evaluation method, as previously used by several researchers (Olaf Helmer-Hirschberg 1967; Lee *et al.* 2013; Räsänen *et al.* 2019). In the Delphi method, a group of relevant independent experts assigns subjective weights to each of the different indicators (Brooks *et al.* 2005; Kumpulainen 2006; El-Zein and Tonmoy 2015). The workshop was arranged with a panel of people from sectors that may be identified to be directly impacted by heat vulnerability, with a specific emphasis on COGG and individual vulnerability. Table 2 indicates the data that was utilized to construct the required indicators to generate the risk factors for exposure and sensitivity, along with their assigned weights.

3.3.6 Generating 2D maps of UHV

Once the weights were decided in the workshop with stakeholders and relevant people, we generated the index maps with multiple indicators and assigned weightings. These were then integrated into a composite measure of population sensitivity to risk (Rinner *et al.* 2010). The processing of weights and generating of indicators was done in GIS software: ArcMap and CommunityViz. CommunityViz plugin represents a group of extensions to ArcGIS software. This plugin is widely used in applications of urban planning and land use/land cover planning (CommunityViz Urban Analytics for Planners 2021). The layers were segregated using the suitability wizard tool in the CommunityViz plugin. The suitability wizard tool utilized given weights to each indicator and merged the layers by providing a final output map. Later the images were composited in ArcGIS to construct the final UHV maps.

4. Results

4.1 Heat exposure maps

The UHI maps generated from Landsat-8 and aerial photos helped to identify hotspots in the city and nearby areas. These hotspots were characterized by less vegetation cover and increased bare land coverage or high building and road density. Figure 4 shows the UHI map for the date 15 December 2017, as seen from the Landsat-8 satellite for COGG. We generated similar maps for 12 December 2016, 11 November 2017, and 1 September 2018 and merged these to generate our

Table 2. Indicators and assigned ranks (source: modified from Roös et al. 2021).

Detriment	Indicators	Weights/Rank
<i>Population sensitive to heat</i>		
Childhood <5	The proportion of children <5 over the total population	2/10
Elderly >65	The proportion of residents >65 over the total population	4/10
Ill-health/people with disabilities (%)	The proportion of ill health people over the total population	2/10
ABS SEIFA	The proportion of people over the total population	1/10
People taking medication	The proportion of people over the total population	0.5/10
Homeless	The proportion of people over the total population	0.5/10
<i>Mobility/accessibility</i>		
Medical facilities	The proportion of parcels/zones beyond a certain distance (parcels beyond the range of 400 m)	3/10
Shopping centres/cinemas	The proportion of parcels/zones beyond a certain distance (parcels beyond the range of 400 m)	1/10
Community centre/care	The proportion of parcels/zones beyond a certain distance (parcels beyond the range of 400 m)	1/10
Public transport – bus stops/train stops	The proportion of parcels/zones beyond a certain distance (parcels beyond the range of 400 m)	1/10
Open spaces	The proportion of parcels/zones beyond a certain distance (parcels beyond the range of 400 m)	1/10
Vegetation green spaces	The proportion of parcels/zones beyond a certain distance (parcels beyond the range of 400 m)	1/10
<i>Spatial locations prone to heat</i>		
Hotspots (Urban Heat Island)	The proportion of residential parcels with higher UHI zones	4/10
Impervious surface per cent (%)	The proportion of area covered by roads	3/10
Enhanced Vegetation Index (EVI)	The proportion of residential parcels with higher EVI zones	3/10

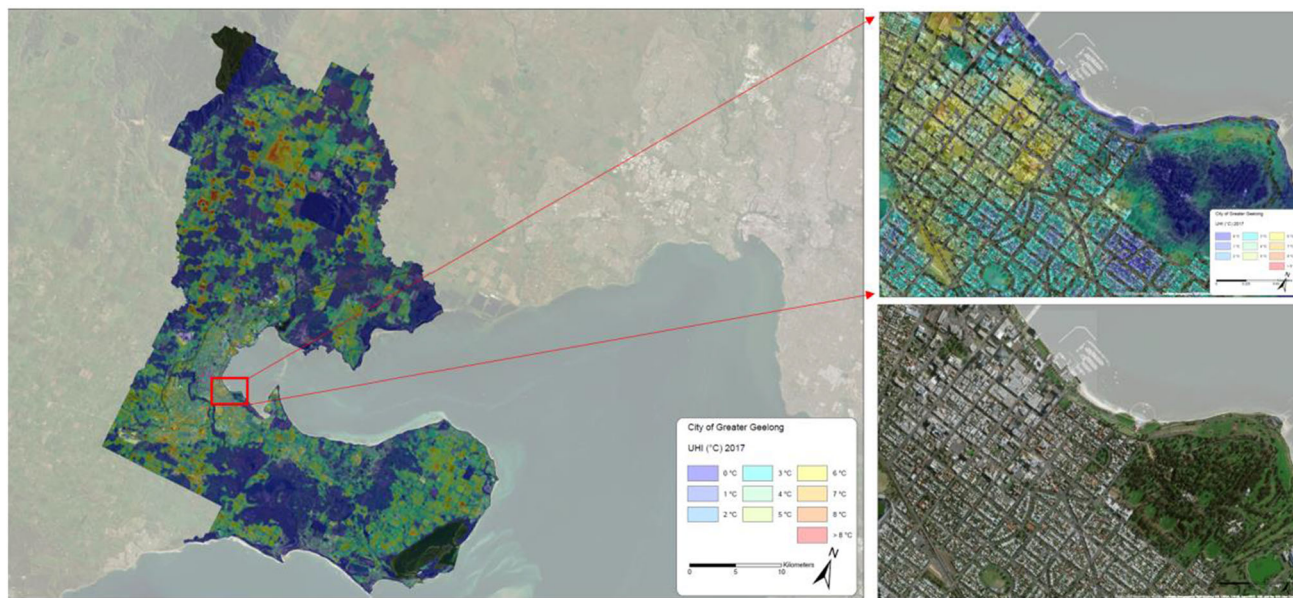


Figure 4. Landsat-8 based UHI map, dated 15 December 2017.

heat exposure maps. Figure 4 further illustrates the map as seen for UHI. We further zoomed the map to highlight hotspots in the inner Central Business

Area (CBA) of COGG. Figure 4 depicts the bare land or land possessing relatively no vegetation having a UHI of 6°C or over, whereas green zones

indicate lower UHI values. In some cases, we also found that the areas or zones reserved for vegetation had higher UHI values, which can be further corroborated by site inspection evidence that north hemisphere-planted perennial grasses covering the reserve zones may be at the end of peak living season as per grass phenology. It is known that grasses are not green the whole year rather, these follow a certain life cycle called phenology, whereas these are greener at their peak of the season. This pattern is particularly evident in Australia, where a mix of northern hemisphere perennial green grasses are used extensively by municipalities across but that is increasingly mixed with native Australian often brown-coloured grasses in decorative and less-intensive-play contexts, wherein they are naturally across the year a mix of green to being to brown in their colour characteristics irrespective of the season and or rainfall.

4.2 Population sensitivity

For risk maps, a particular population was highlighted to be most vulnerable to heat risk. Figure 5 indicates the population sensitivity map generated from indicators for population sensitivity and

assigned weights. Moreover, the following figures were based on the meshblock scale that graphically shows a proportion of a sensitive group of people. The results from the modelling shown in figure 5 indicate that the majority of risk areas are away from the CBA, concluding that most of the elderly people are living further away from the central city. The overall rank goes from 0 to 1. Hence, with 0 being the lowest rank and 1 being the highest rank, it means 1 shows areas with the most sensitive zones and 0 illustrates areas with the least sensitive zones.

4.3 Accessibility/mobility map

Figure 6 depicts the accessibility/mobility maps for COGG. This map highlights the areas of easier access to people for obtaining thermal comfort or medical help in case of extreme temperatures or prolonged heatwave events.

4.4 Urban Heat Vulnerability (UHV)

Our applied analysis involves an approach similar to academic research methodologies used to map social vulnerability to environmental hazards.

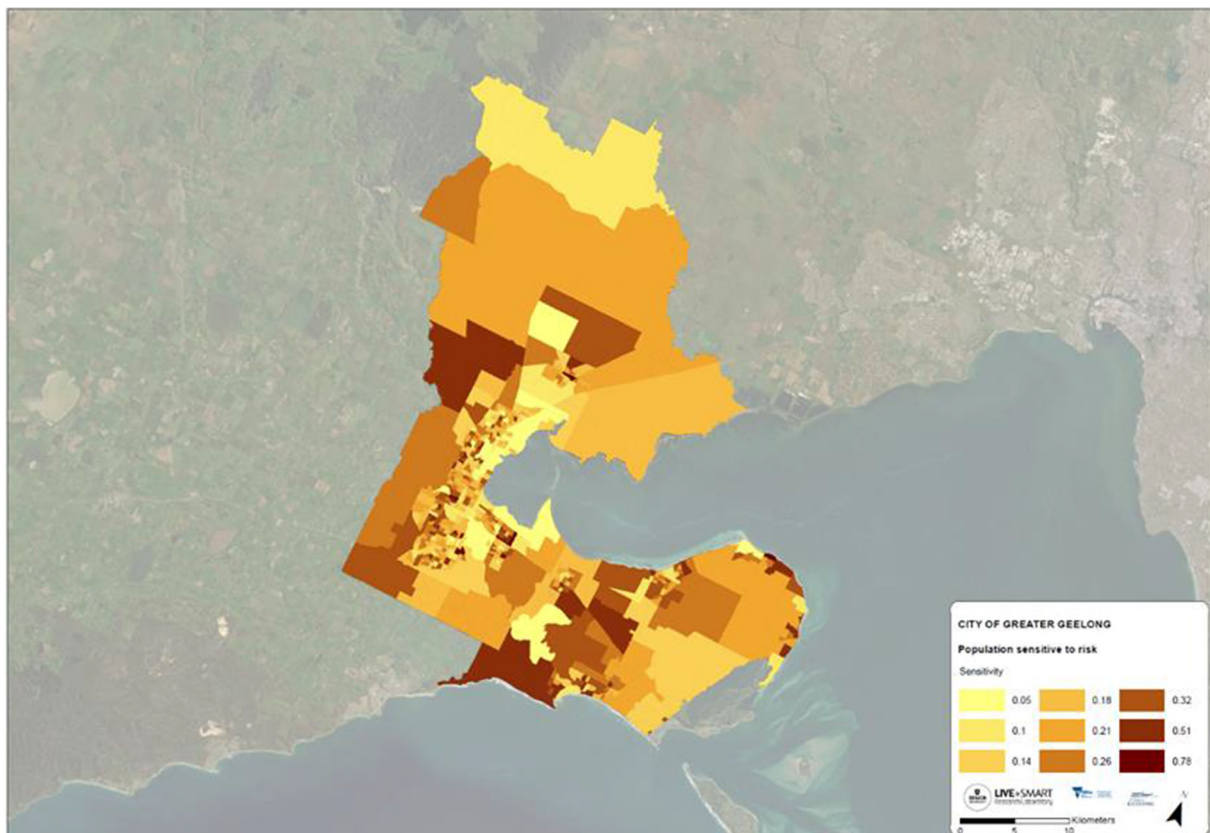


Figure 5. Population sensitivity map Geelong.

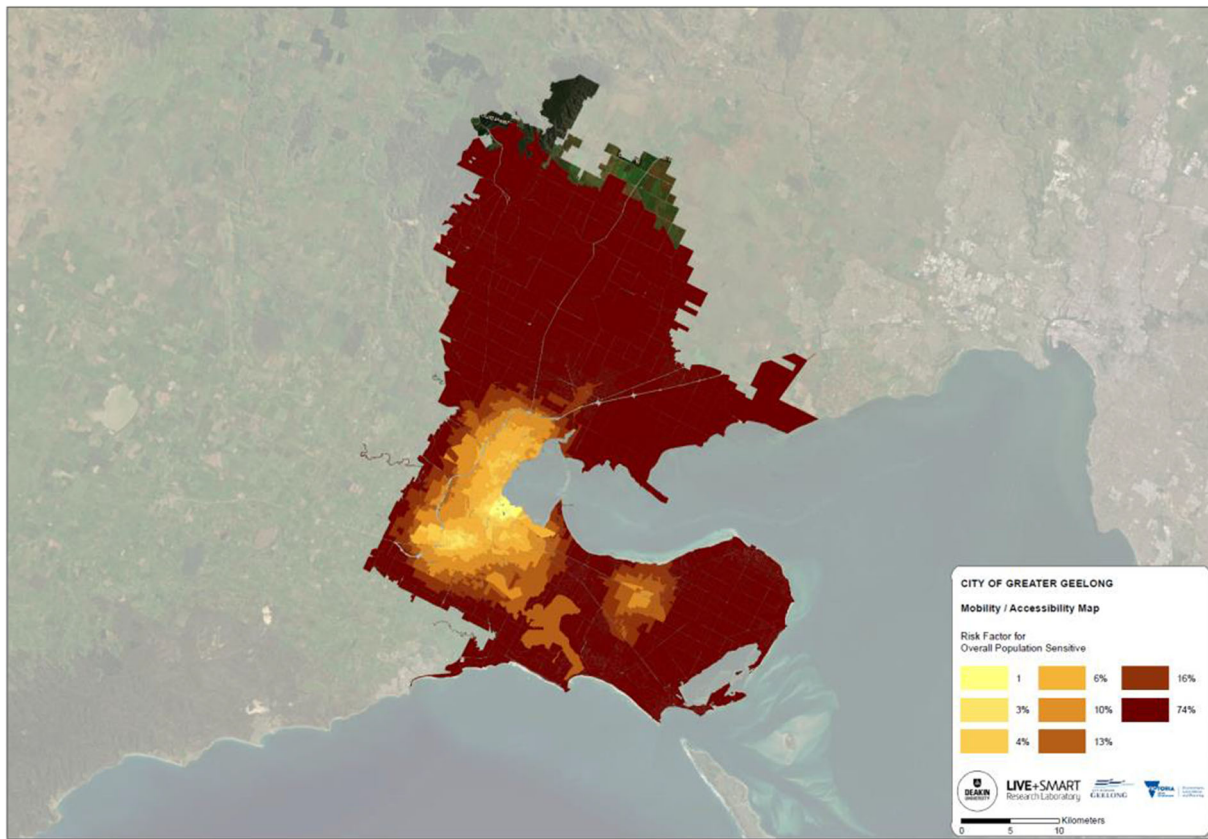


Figure 6. Accessibility/mobility map.

Figure 7 shows the UHV map for COGG. Figure 7 highlights the zones with selected indicators and given weights. The assigned weights can be changed as per further analysis and options. Figure 7 indicates the high-risk zones. The scale for UHV goes from 0 to 1, where values equal to 0.4 or less indicate no risk, values above or equal to 0.5 represent a low risk, values above or equal to 0.6 represent a low-medium risk, values above or equal to 0.7 represent a medium risk, values above or equal to 0.8 represent a high risk, and values above or equal to 0.8 represent a very high risk. Figure 7 shows the current status of COGG as per heat vulnerability risk for a selected sensitive group of population. It can be further observed that most of the zones in COGG are at no risk or less risk; however, some of the spots indicate medium to high risk due to a higher proportion of the sensitive population and increased exposure to heat when these maps are generated from heat exposure, population and accessibility maps. These areas of medium to high risk could also be areas with less vegetation coverage or tree coverage, as greenness plays a vital role in diminishing the effects of heat or extreme temperatures. The results were

provided to the council, as the work was part of the project. Council further verified and ground-truthed the model and results.

4.5 Relationship of UHI with population and building density

The UHI maps were further correlated with the total population, population density, and building density. Figure 8 illustrates the maps and graphs generated for UHI per meshblock, population per meshblock, population density per meshblock, building density per meshblock, and their relationship with UHI measurements. The correlation graphs indicate a significant direct relationship of UHI with population and building density, as the p -value indicates < 0.01 . The results further support the statement that the higher the population density, the higher is the building density, and so it leads to higher UHI.

High building density indicates dense settlements, high impervious surface per cent, and therefore low vegetation cover leading to higher anthropogenic heat and ultimately high UHI intensity in those particular zones. Residential

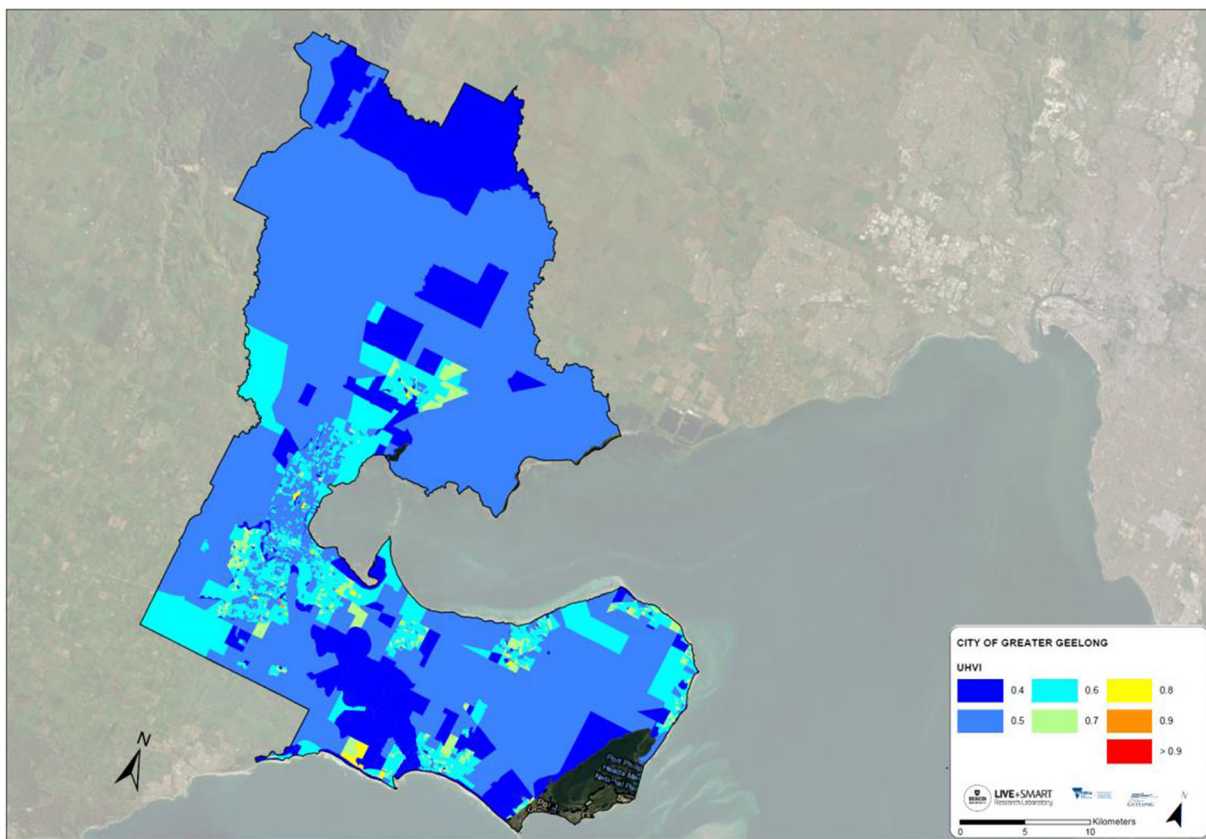


Figure 7. UHV map (source: modified from Roös *et al.* 2021).

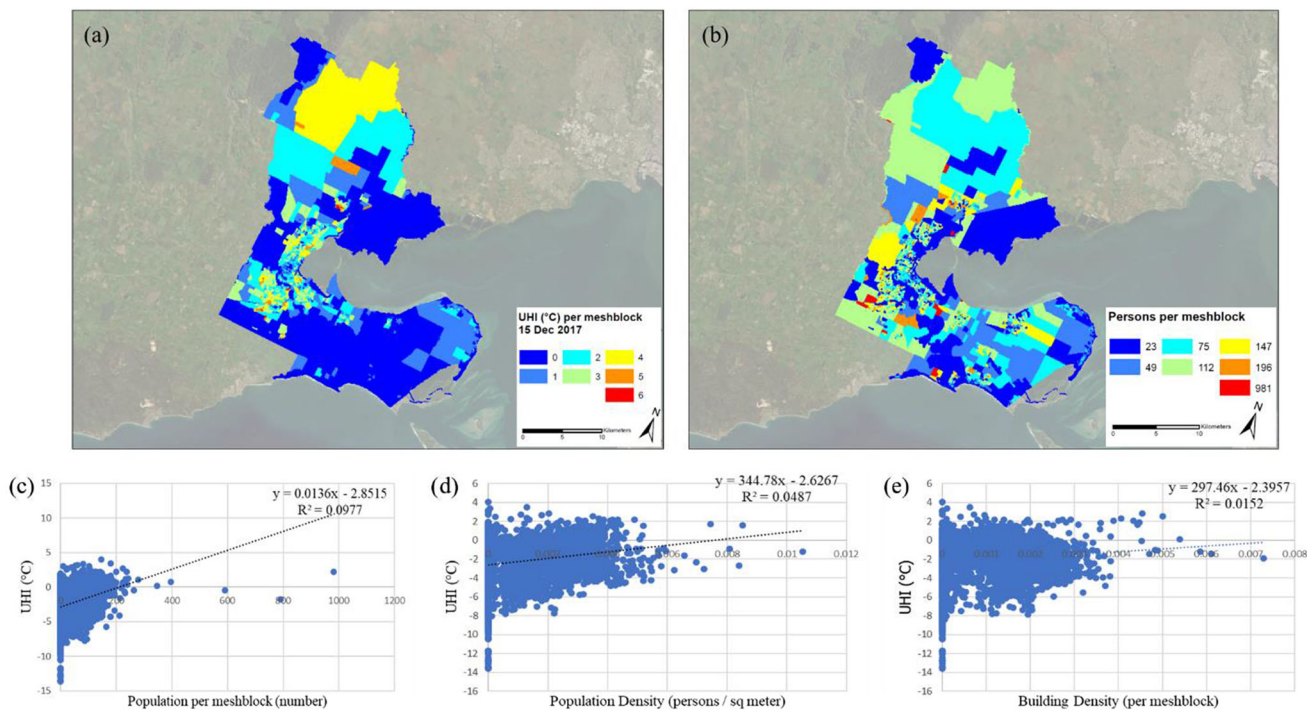


Figure 8. (a) Map representing UHI per meshblock as of 15 December 2017; (b) Map representing persons per meshblock as of ABS 2016 Census data; (c) Graph showing correlation between UHI measurements against population per meshblock; (d) Graph showing correlation between UHI measurements against population density (persons per sq. meter); (e) Graph showing a correlation between UHI measurements against building density per meshblock.

areas with less population density and low building density with higher spatial distribution contribute to the UHI effect. Literature also supports our results, where it has been observed that higher population density results in higher anthropogenic heat due to dense settlements and a high percentage of impervious surfaces.

5. Discussion

During the 20th century, temperatures increased significantly faster in cities compared to nearby rural areas due to the urban heat island effect. The transformation of native landscapes into dense urban settlements possessing heat-retaining impervious surfaces and building materials that inhibit night-time cooling is the most significant anthropogenic driver of urban climate change in cities around the world. Warmer baseline temperatures in cities are further elevated by extreme heat events (EHEs) or heat waves, which are projected to strike with increasing frequency and intensity in the 21st century.

Our analysis applies a similar methodology used in other academic research projects to map social vulnerability to environmental hazards. We highlighted areas with the highest risk and vulnerability to extreme heat, considering the vulnerability factors in this analysis. Taking reference to IPCC report data and scenarios, heat waves were projected to increase in frequency, duration, and intensity. In this research, the vulnerability maps were projected for 2040, 2070, and 2100 recognizing population growth in the region and using temperature projections drawn from the IPCC and CSIRO and respective UHI changes.

Climate change is one of the most complex issues of the 21st century. Even though there is a consensus about the urgency of taking action at the city level, planning and implementation of adaptation and resilience measures are advancing slowly. The lack of data and information to support the planning process is often mentioned as a factor hampering the adaptation processes in cities. In this paper, we developed and tested a methodology for heat stress vulnerability and risk assessment at the neighbourhood scale to support designers, planners, and decision-makers in developing and implementing adaptation strategies and measures at the local level. The methodology combined high-resolution spatial information and crowd-sourcing geospatial data to develop sensitivity, adaptive

capacity, vulnerability, exposure, and risk indicators. The methodology was then tested on the urban fabric of the COGG municipality in Australia. Our results show that different vulnerability and risk values correspond to different typologies of urban areas. Furthermore, the possibility of combining high-resolution information provided by the indicators and land use categories is of great importance to support the adaptation planning process. We also argue that the methodology is flexible enough to be applied in different contexts.

From the literature, it was established that most studies had opted to use temperature maps instead of using UHI maps. From this study, it is apparent that some critical issues may be overlooked when this is the case. For instance, according to the results obtained, it was evident that some areas of COGG municipalities revealed few sensitive groups of people, especially the elderly. Coupling this result with the mobility map, it is easier to understand the morphology of population dynamics in cities. With UHV, it becomes even clearer not only how the urban population dynamics are but how much could be moulded to render more liveable urban fabrics. On this, such information becomes critical, especially for urban planners regarding adopting greener infrastructural investments and helping in providing UHI mitigation measures in urban areas. From the study, it was evident that areas of 'no risk' or 'less risk' had a higher proportion of the sensitive population, thus supporting the proposition of having increased greener spaces. This finding corresponds with the argument by Aram *et al.* (2019), who also noted that green spaces have the propensity to reduce the impacts of UHI and offer safe havens for surrounding occupants due to their increased capabilities to influence both the intensity and density of cooling.

Besides helping in planning for both, understanding the UHV is important in helping in determining the locations and distancing of critical urban infrastructures such as health facilities. From the results, it has been observed that areas with less green and those perceived to experience higher UHI have fewer populations. Additionally, with the ongoing trends of the increasing urban population, and the unprecedented changing weather patterns, it would be important to consider prioritizing critical infrastructures, especially in vulnerable urban areas. This could entail further equipping existing health facilities to build capacity for the increasing cases of hospitalizations and

the emergence of heat-related health issues, as noted in an article by the California Environment protection agency. The UHV results obtained in this study further affirm the need for prioritizing certain parts of cities for mitigation by adopting, among others, strategies such as emphasizing urban greening, adopting green building and construction strategies, and adopting modern urban planning models, among other strategies.

Finally, it is noted that UHI studies are site-specific and that results vary in regard to the typology and morphology. With the increasing concerns of urbanization and the associated concerns of health-related impacts on both health and urban comfort, and its socio-economic impacts, there is a growing need for further research in this area, through the use of multi-methodological approaches, as is the case of this study.

6. Limitations

The paper discusses the benefits of integrating remote sensing data in developing the approach to map heat-risk areas to urban residents. The UHI, which is derived from satellite, is called surface urban heat island, and the UHI derived from air temperature is called boundary/canopy Urban Heat Island (Oke 1982). We used surface UHI for our analysis in this research since the available air temperature data were insufficient for the subject study due to limited coverage (only one station covers the whole greater city area). The UHI derived from LST, as seen in satellite images, is dominantly present, particularly during daytime (Ramamurthy *et al.* 2017). LST has, in fact, different physical meanings from surface air temperature; however, they have close and complex relations, and both contribute to building the UHI effect. Generally, under clear sky conditions, larger LST means larger sensible heat flux, resulting in larger surface air temperature and higher urban boundary layer (Arnfield 2003).

The images used in the manuscript were of daytime and summer months. The context of this paper is to analyze risk areas within the city during extreme heat days in summer. Since the available data were daytime, we had to restrict our analysis to daytime temperatures. UHI is a diurnal phenomenon that exists both during the day and night-time (Sidiqui *et al.* 2016; Zhou 2018). Some studies also noticed that the daytime intensities in UHI were significantly higher in magnitude than at

night (Yao *et al.* 2018; Zhou 2018). However, it is recommended to carry out a night-time study for a similar context, which may require additional drone flights, particularly at night-time and respective ground-truthing. In addition to it, the MODIS satellite, on the other hand, may provide diurnal analysis; however, the spatial resolution is coarse (1000 m), which may put a hurdle on subject analysis.

The study did not incorporate satellite-based vegetation (NDVI/EVI) data since vegetation data acquired from the council was detailed, ground-truthed, and up-to-date. In that case, it was not required to process satellite images to calculate vegetation cover for the study area. In addition to it, city elevation was ignored in the subject assessment of UHI, due to no significant variations in topology, since the average elevation of the city is 33 m above sea level (Roös *et al.* 2021). Other data, such as wind data that may have implications on UHI pattern, were not included in the subject assessment due to the lack of availability of these data sets. However, such inclusions are suggested in future studies depending on data availability.

7. UHI risk management

The UHI risk can be managed by introducing more vegetation cover in city areas so that the hotspots can be converted into cool spots. Another measure that can be taken is that the locations which are concentrated with more population of elderly, children, and population higher at risk, should be given access to emergency services. For example, when it is heat stress or heatwave event, the emergency departments should be on call and within the buffer of accessibility of sensitive populations. Moreover, these highlighted risk areas should be accommodated with accessible relief centres, emergency services, and relatively more plantation of trees and vegetation.

8. Conclusion

This research discusses the benefits of integrating remote sensing data in developing the approach to map heat-risk areas to urban residents. In literature, the UHI, which is mapped from the satellite, is called a surface Urban Heat Island. The air temperature data was not sufficient for the sit; thus, in this study, we utilized SUHI index maps. The satellite-based temperature maps not only provide

us the liberty of going back in time but also offers a great range of coverage. It is factual that air temperature is not the same as surface temperature; however, the surface temperatures also contribute to developing the UHIs in the cities these are dominant, particularly in the daytime. This study is based on SUHI index maps; however, the approach utilized can also be copied if air temperature UHI is available for the selected site. This research presents a comprehensive and detailed study; it also helps in identifying the key indicators of heat risk, whether in population, mobility, or spatial variance. During the 20th century, temperatures increased significantly faster in cities compared to nearby rural areas due to the Urban Heat Island (UHI) effect. Despite some limitations, the findings of this study provide useful information for mapping and monitoring urban heat vulnerability risk zones, especially during summer. The risk factors used for heat exposure, sensitivity, and adaptive capacity in the multiple studies used different approaches. In this study, we proposed a simple and easy-to-follow methodology. Moreover, we proposed to utilize UHI maps instead of utilizing direct land surface temperature maps. The different risk factors identified in our literature appraisal largely used simple temperature maps to identify heat exposure in urban zones. Where UHI was one phenomenon and may cause hotspots in urban areas, it was very evident that it caused particular locations to result in a relatively higher risk than in other zones within the same urban polygon.

Acknowledgements

The work was completed as part of a funded project titled ‘*Climate Change & Heatwave Project: Identification of High-Risk areas for the City of Greater Geelong*’ (2020) between Deakin University and the Department of Environment, Land, Water and Planning (DELWP) and City of Greater Geelong (COGG) in Australia. The authors want to acknowledge the support from the Live+Smart Research Laboratory, School of Architecture and Built Environment, Deakin University.

Author statement

PS: Numerical modelling, mapping, analysis, interpretation of results, and drafting of the

original manuscript. PBR: Data collection and interpretation of results and drafting the original manuscript. MH: Data collection and interpretation of results and drafting the original manuscript. DJ: Data analysis and interpretation, drafting the revised manuscript. ED and AJ: Analysis and drafting of the revised manuscript. BJR and MAURT: Field data collection, ground-truthing, drafting the revised manuscript. AS: Field data collection and ground-truthing. AAS, NAK and MI: Data analysis and manuscript revision.

References

- Aram F, García E H, Solgi E and Mansournia S 2019 Urban green space cooling effect in cities; *Heliyon* **5**(4) 01339, <https://doi.org/10.1016/j.heliyon.2019.e01339>.
- Arnfield A J 2003 Two decades of urban climate research: A review of turbulence, exchanges of energy and water, and the urban heat island; *Int. J. Climatol.* **23**(1) 1–26, <https://doi.org/10.1002/joc859>.
- Black Saturday death toll lowered – ABC News 2009, <https://www.abc.net.au/news/2009-03-30/black-saturday-death-toll-lowered/1635324>.
- BOM (Bureau of Meteorology) 2017 *About the Heatwave Service*, <http://www.bom.gov.au/australia/heatwave/about.shtml>.
- BOM (Bureau of Meteorology) 2018 *Annual climate statement*, <http://www.bom.gov.au/climate/current/annual/aus/2018/>.
- Brooks N, Adger W N and Kelly P M 2005 The determinants of vulnerability and adaptive capacity at the national level and the implications for adaptation; *Global Environ. Change* **15**(2) 151–163, <https://doi.org/10.1016/j.gloenvcha.2004.12.006>.
- Chow W T L, Chuang W C and Gober P 2012 Vulnerability to extreme heat in Metropolitan Phoenix: Spatial, temporal, and demographic dimensions; *Prof. Geogr.* **64**(2) 286–302, <https://doi.org/10.1080/00330124.2011.600225>.
- Chowienzyk K, McCarthy M P, Hollis D, Dyson E, Lee M and Coley D 2020 Estimating and mapping urban heat islands of the UK by interpolation from the UK Met Office observing network; *Build. Serv. Eng. Res. Technol.* **41** 521–543, <https://doi.org/10.1177/0143624419897254>.
- Chuang W C and Gober P 2015 Predicting hospitalization for heat-related illness at the census tract level: accuracy of a generic heat vulnerability index in Phoenix, Arizona (USA); *Environ. Health Perspect.* **123**(6) 606, <https://doi.org/10.1289/ehp.1307868>.
- Clayton R 2021 Thinking of moving to Geelong? This framework will set the future of the city; *ABC News*, <https://www.abc.net.au/news/2021-05-25/government-plan-for-geelong-cbd-future-as-house-population-boom/100156728>.
- CommunityViz Urban Analytics for Planners 2021, <https://communityviz.city-explained.com/>.
- CSIRO (The Commonwealth Scientific and Industrial Research Organisation) 2011 *Climate Change: Science and Solutions for Australia*, <https://www.csiro.au/en/>

- research/environmental-impacts/climate-change/climate-change-science-and-solutions.
- DHS J 2009 *Heatwave in Victoria: An assessment of health impacts*; Department of Health VIC Australia, <https://www.health.vic.gov.au/publications/january-2009-heatwave-in-victoria-an-assessment-of-health-impacts>.
- Dimitrov M S, Dimitrov A, Popov M, Dimitrov S, Popov A and Iliev M 2020 Mapping and assessment of urban heat island effects in the city of Sofia, Bulgaria through integrated application of remote sensing, unmanned aerial systems (UAS) GIS; *SPIE Int. Soc. Opt. Photonics* **11524** 459–470, <https://doi.org/10.1117/12.2571967>.
- El-Zein A and Tonmoy F N 2015 Assessment of vulnerability to climate change using a multi-criteria outranking approach with application to heat stress Sydney; *Ecol. Indic.* **48** 207–217, <https://doi.org/10.1016/j.ecolind.2014.08.012>.
- Epstein S and Atul K 2006 Heatwave/hyperthermia. In *Handbook of Bioterrorism and Disaster Medicine*; Springer, Boston, MA, pp. 73–77.
- Fastest Growth Region Needs Faster Infrastructure Delivery – G21 2020, <https://g21.com.au/news/fastest-growth-region-needs-faster-infrastructure-delivery/>.
- Galloa K P, McNabb A L, Karlb T R and Brown J F 1993 The Use of NOAA AVHRR Data for Assessment of the Urban Heat Island Effect; *J. Appl. Meteorol. Climatol.* **32(5)** 899–908, [https://doi.org/10.1175/1520-0450\(1993\)032%3c0899:TUONAD%3e2.0.CO;2](https://doi.org/10.1175/1520-0450(1993)032%3c0899:TUONAD%3e2.0.CO;2).
- Grose M R 2015 Comparison of various climate change projections of eastern Australian rainfall; *Austr. Meteorol. Oceanogr. J.* **65** 67–84.
- Harlan S L, Brazel A J, Prashad L, Stefanov W L and Larsen L 2006 Neighborhood microclimates and vulnerability to heat stress; *Soc. Sci. Medic.* **63(11)** 2847–2863, <https://doi.org/10.1016/J.SOCSCIMED.2006.07.030>.
- Heaton M J, Sain S R, Greasby T A, Uejio C K, Hayden M H, Monaghan A J, Boehnert J, Sampson K, Banerjee D, Nepal V and Wilhelmi O V 2014 Characterizing urban vulnerability to heat stress using a spatially varying coefficient model; *Spat. Spatio-Temporal Epidemiol.* **8** 23–33, <https://doi.org/10.1016/J.SSTE.2014.01.002>.
- Heatwave Management: Reducing the Risk to Public Health | Victorian Auditor-General's Office 2014, <https://www.audit.vic.gov.au/report/heatwave-management-reducing-risk-public-health?section>.
- Heaviside C, Macintyre H and Vardoulakis S 2017 The Urban Heat Island: Implications for Health in a Changing Environment; *Curr. Environ. Health Rep.* **4(3)** 296–305, <https://doi.org/10.1007/s40572-017-0150-3>.
- Hélia C and Graham F 2015 Economic costs of heat and flooding in cities: Cost and economic data for the European Clearinghouse databases; London European Union, https://climate-adapt.eea.europa.eu/metadata/publications/economic-costs-of-heat-and-flooding-in-cities/ramses_2015_economic-costs-of-climate-change-in-european-cities.pdf.
- Huang G, Zhou W and Cadenasso M L 2011 Is everyone hot in the city? Spatial pattern of land surface temperatures, land cover and neighborhood socio-economic characteristics in Baltimore, MD; *J. Environ. Manag.* **92(7)** 1753–1759, <https://doi.org/10.1016/j.jenvman.2011.02.006>.
- IPCC 2021 Climate Change 2021: The Physical Science Basis Contribution of Working Group I to the Sixth Assessment Report of the Intergovernmental Panel on Climate Change Cambridge University Press, <https://www.ipcc.ch/report/ar6/wg1/downloads/report/IPCC.AR6.WGI.Citation.pdf>.
- Keeratikasikorn C and Bonafoni S 2018 Urban Heat Island analysis over the land use zoning plan of Bangkok by means of Landsat 8 Imagery; *Remote Sens.* **10(3)** 440, <https://doi.org/10.3390/rs10030440>.
- Keramitsoglou I, Kiranoudis C T, Ceriola G, Weng Q and Rajasekar U 2011 Identification and analysis of urban surface temperature patterns in Greater Athens, Greece, using MODIS imagery; *Remote Sens. Environ.* **115(12)** 3080–3090, <https://doi.org/10.1016/j.rse.2011.06.014>.
- Kovats R S and Kristie L E 2006 Heatwaves and public health in Europe; *European J. Public Health* **16(6)** 592–599, <https://doi.org/10.1093/eurpub/ckl049>.
- Kumar P, Geneletti D and Nagendra H 2016 Spatial assessment of climate change vulnerability at city scale: A study in Bangalore, India; *Land Use Policy* **58** 514–532, <https://doi.org/10.1016/J.LANDUSEPOL.2016.08.018>.
- Kumpulainen S 2006 Vulnerability concepts in hazard and risk assessment; *Geol. Surv. Finland* **42** 65–74, <https://citeseerx.ist.psu.edu/viewdoc/download?doi=10.1.1.571.7244&rep=rep1&type=pdf>.
- Lai L W and Cheng W L 2009 Air quality influenced by urban heat island coupled with synoptic weather patterns; *Sci. Total Environ.* **407(8)** 2724–2733, <https://doi.org/10.1016/J.SCITOTENV.2008.12.002>.
- Lee G, Jun K S and Chung E S 2013 Integrated multi-criteria flood vulnerability approach using fuzzy TOPSIS and Delphi technique; *Nat. Hazards Earth Syst. Sci.* **13(5)** 1293–1312, <https://doi.org/10.5194/NHESS-13-1293-2013>.
- Lemonsu A, Vigié V, Daniel M and Masson V 2015 Vulnerability to heat waves: Impact of urban expansion scenarios on urban heat island and heat stress in Paris (France); *Urban Clim.* **14** 586–605, <https://doi.org/10.1016/J.UCLIM.2015.10.007>.
- Li Z-L, Tang B-H, Wu H, Ren H, Yan G, Wan Z, Trigo I F and Sobrino J A 2013 Satellite-derived land surface temperature: Current status and perspectives; *Remote Sens. Environ.* **131** 14–37, <https://doi.org/10.1016/j.rse.2012.12.008>.
- Li H, Meier F, Lee X, Chakraborty T, Liu J, Schaap M and Sodoudi S 2018 Interaction between urban heat island and urban pollution island during summer in Berlin; *Sci. Total Environ.* **636** 818–828, <https://doi.org/10.1016/J.SCITOTENV.2018.04.254>.
- Li Y Y, Liu Y, Ranagalage M, Zhang H and Zhou R 2020 Examining land use/land cover change and the summertime surface urban heat island effect in fast-growing Greater Hefei, China: Implications for sustainable land development; *ISPRS Int. J. Geo-Infor.* **9(10)** 568, <https://doi.org/10.3390/ijgi9100568>.
- Lin S, Hsu W H, Van Zutphen A R, Saha S, Lubber G and Hwang S A 2012 Excessive heat and respiratory hospitalizations in new york state: Estimating current and future public health burden related to climate change; *Environ. Health Persp.* **120(11)** 1571, <https://doi.org/10.1289/ehp.1104728>.
- Masson-Delmotte V P, Zhai H O, Pörtner D, Roberts J, Skea, Shukla P R, Pirani A, Moufouma-Okia W, Péan C, Pidcock R, Connors S, Matthews J B R, Chen Y, Zhou X, Gomis M I, Lonnoy E, Maycock T, Tignor M and Waterfield T 2018 Global Warming of 1.5°C. An IPCC Special Report on the impacts of global warming of 1.5°C above pre-industrial

- levels and related global greenhouse gas emission pathways, in the context of strengthening the global response to the threat of climate change, sustainable development, and efforts to eradicate poverty; IPCC Press, <https://www.ipcc.ch/site/assets/uploads/sites/2/2019/06/SR15.Full.Report.High.Res.pdf>.
- Mathew A, Sreekumar S, Khandelwal S and Kumar R 2019 Prediction of land surface temperatures for surface urban heat island assessment over Chandigarh city using support vector regression model; *Sol. Energy* **186** 404–415, <https://doi.org/10.1016/J.SOLENER.2019.04.001>.
- Meerow S and Newell J P 2017 Spatial planning for multifunctional green infrastructure: Growing resilience in Detroit; *Landscape Urban Plan.* **159** 62–75, <https://doi.org/10.1016/J.LANDURBPLAN.2016.10.005>.
- Méndez-Lázaro P, Muller-Karger F E, Otis D, McCarthy M J and Rodríguez E 2018 A heat vulnerability index to improve urban public health management in San Juan; *Puerto Rico Int. J. Biometeorol.* **62**(5) 709–722, <https://doi.org/10.1007/s00484-017-1319-z>.
- Menut L 2000 Measurements and modelling of atmospheric pollution over the Paris area: An overview of the ESQUIF Project; *Ann. Geophys.* **18**(11) 1467–1481, <https://doi.org/10.1007/S00585-000-1467-Y>.
- Oke T R 1982 The energetic basis of the urban heat island; *Quart. J. Roy. Meteorol. Soc.* **108**(455) 1–24, <https://doi.org/10.1002/qj.49710845502>.
- Olaf Helmer-Hirschberg 1967 Analysis of the Future: The Delphi Method; *RAND Cooperation Objective Analysis Effect Solutions*, <https://www.rand.org/pubs/papers/P3558.html>.
- Raalte L V, Nolan M, Thakur P, Xue S and Parker N 2012 Economic assessment of the Urban Heat Island Effect Melbourne; AECOM Australia Pty Ltd, <https://www.melbourne.vic.gov.au/sitecollectiondocuments/eco-assessment-of-urban-heat-island-effect.pdf>.
- Ramamurthy P, Li D and Bou-Zeid E 2017 High-resolution simulation of heatwave events in New York City; *Theoret. Appl. Climatol.* **128**(1–2) 89–102, <https://doi.org/10.1007/S00704-015-1703-8>.
- Räsänen A, Heikkinen K, Piila N and Juhola S 2019 Zoning and weighting in urban heat island vulnerability and risk mapping in Helsinki, Finland; *Reg. Environ. Change* **19**(5) 1481–1493, <https://doi.org/10.1007/s10113-019-01491-x>.
- Reid C E, O'Neill M S, Gronlund C J, Brines S J, Brown D G, Diez-Roux A V and Schwartz J 2009 Mapping community determinants of heat vulnerability; *Environ. Health Persp.* **117**(11) 1730–1736, <https://doi.org/10.1289/ehp.0900683>.
- Rinner C, Patychuk D, Bassil K, Nasr S, Gower S and Campbell M 2010 The role of maps in neighborhood-level heat vulnerability assessment for the city of Toronto; *Cartogr. Geogr. Inf. Sci.* **37**(1) 31–44, <https://doi.org/10.1559/152304010790588089>.
- Rizvi S H, Alam K and Iqbal M J 2019 Spatio-temporal variations in urban heat island and its interaction with heat wave; *J. Atmos. Sol.-Terr. Phys.* **185** 50–57, <https://doi.org/10.1016/J.JASTP.2019.02.001>.
- Roös P B, Sidiqi P, Herron M, Jones D S and Duncan E 2021 Climate Change and Heatwave Project: Identification of high-risk areas across the City of Greater Geelong Climate Change and Heatwave Project: Identification of high-risk areas across the City of Greater Geelong, A Report to the Department of Environment, Land, Water and Planning (DELWP) and the City of Greater Geelong (COGG), Live+Smart Research Laboratory, School of Architecture & Built Environment, Deakin University, Geelong, VIC, <https://geelongaustralia.com.au/environment/documents/item/8d07ddbc8d1be5a.aspx>.
- Saeed F, Schleussner C F and Ashfaq M 2021 Deadly heat stress to become commonplace across South Asia already at 15°C of Global Warming; *Geophys. Res. Lett.* **48**(7), <https://doi.org/10.1029/2020GL091191>.
- Sanchez L and Reames T G 2019 Cooling Detroit: A socio-spatial analysis of equity in green roofs as an urban heat island mitigation strategy; *Urban For. Urban Green.* **44** 126331, <https://doi.org/10.1016/j.ufug.2019.04.014>.
- Schatz J and Kucharik C J 2015 Urban climate effects on extreme temperatures in Madison, Wisconsin, USA; *Environ. Res. Lett.* **10**(9) 094024, <https://doi.org/10.1088/1748-9326/10/9/094024>.
- Sharma A, Woodruff S, Budhathoki M, Hamlet A F, Chen F and Fernando H J S 2018 Role of green roofs in reducing heat stress in vulnerable urban communities – a multidisciplinary approach; *Environ. Res. Lett.* **13**(9) 094011, <https://doi.org/10.1088/1748-9326/aad93c>.
- Sidiqi P 2019 Cities from space: Influence of rural to urban gradients on remote sensing of urban heat island Sydney (Doctoral dissertation), <https://opus.lib.uts.edu.au/handle/10453/136130>.
- Sidiqi P, Huete A and Devadas R 2016 Spatio-temporal mapping and monitoring of Urban Heat Island patterns over Sydney, Australia using MODIS and Landsat-8; *4th International Workshop on Earth Observation and Remote Sensing Applications, EORSA*, pp. 217–221, <https://doi.org/10.1109/EORSA.2016.7552800>.
- Sidiqi P, Tariq M A U R and Ng A W M 2022 An Investigation to identify the effectiveness of socioeconomic, demographic, and buildings characteristics on Surface Urban Heat Island patterns; *Sustainability* **14**(5) 2777, <https://doi.org/10.3390/su14052777>.
- Tomlinson C J, Chapman L, Thornes J E and Baker C J 2011 Including the urban heat island in spatial heat health risk assessment strategies: A case study for Birmingham, UK; *Int. J. Health Geogr.* **10**(1) 1–14, <https://doi.org/10.1186/1476-072X-10-42>.
- Uejio C K, Wilhelmi O V, Golden J S, Mills D M, Gulino S P and Samenow J P 2011 Intra-urban societal vulnerability to extreme heat: The role of heat exposure and the built environment, socioeconomics, and neighborhood stability; *Health Place* **17**(2) 498–507, <https://doi.org/10.1016/J.HEALTHPLACE.2010.12.005>.
- Vaidyanathan A, Malilay J, Schramm P and Saha S 2020 Heat-related deaths – United States, 2004–2018; *MMWR Morbidity and Mortality Weekly Report* **69**(24) 729–734, <https://doi.org/10.15585/mmwr.mm6924a1>.
- Vargo J, Stone B, Habeeb D, Liu P and Russell A 2016 The social and spatial distribution of temperature-related health impacts from urban heat island reduction policies; *Environ. Sci. Policy* **66** 366–374, <https://doi.org/10.1016/j.envsci.2016.08.012>.
- Voelkel J, Hellman D, Sakuma R and Shandas V 2018 Assessing vulnerability to urban heat: A study of disproportionate heat exposure and access to refuge by

- socio-demographic status in Portland, Oregon; *Int. J. Environ. Res. Public Health* **15**(4) 640, <https://doi.org/10.3390/ijerph15040640>.
- Voogt J A and Oke T R 2003 Thermal remote sensing of urban climates; *Remote Sens. Environ.* **86**(3) 370–384, [https://doi.org/10.1016/S0034-4257\(03\)00079-8](https://doi.org/10.1016/S0034-4257(03)00079-8).
- Walter I 2016 *The Infrastructure Finance Challenge*; Open Book Publishers, <https://www.openbookpublishers.com/product/544>.
- Wang W, Liu K, Tang R and Wang S 2019 Remote sensing image-based analysis of the urban heat island effect in Shenzhen, China; *Phys. Chem. Earth* **110** 168–175, <https://doi.org/10.1016/J.PCE.2019.01.002>.
- Western Geelong Growth Area Precinct – VPA 2022, <https://vpa.vic.gov.au/project/western-geelong-growth-area/>.
- Western Geelong Growth Area Precinct 2022, <https://www.geelongaustralia.com.au/futuregrowth/default.aspx>.
- Yang Q, Huang X and Tang Q 2019 The footprint of urban heat island effect in 302 Chinese cities: Temporal trends and associated factors; *Sci. Total Environ.* **655** 652–662, <https://doi.org/10.1016/j.scitotenv.2018.11.171>.
- Yao R, Wang L, Huang X, Zhang W, Li J and Niu Z 2018 Interannual variations in surface urban heat island intensity and associated drivers in China; *J. Environ. Manag.* **222** 86–94, <https://doi.org/10.1016/j.jenvman.2018.05.024>.
- Zaheer A K and Elahee K E 2014 Exploring the Urban Heat Island (UHI) Effect in Port Louis, Mauritius; *Univ. Mauritius Res. J.*, https://www.researchgate.net/publication/327954662_Exploring_the_Urban_Heat_Island_UHI_Effect_in_Port_Louis_Mauritius.
- Zhou D 2018 Satellite remote sensing of Surface Urban Heat Islands: progress, challenges, and perspectives; *Rem. Sens.* **11**(1) 48, <https://doi.org/10.3390/rs11010048>.

Corresponding editor: APARNA SHUKLA